UDC669.14.018.25/.27:629.114.6

Recent Advances in Ultrahigh-Strength Sheet Steels for Automotive Structural Use

Kazumasa Yamazaki*1
Masaru Oka*3
Hideaki Yasuda*4
Yaichiro Mizuyama*2
Hiroshi Tsuchiya*4

Abstract:

Findings obtained to date are summarized about the properties of ultrahigh-strength sheet steels that are gaining importance as reinforcement members of automobile bodies. Their formability, delayed fracture characteristics, spot weldability, and fatigue strength are described in detail in relation to microstructure, chemical composition, and manufacturing conditions. Formability, in particular, is closely related to microstructural homogeneity and can be significantly improved by improving it. Delayed fracture is related to the amount of retained austenite and can be prevented by reducing it. Ultrahigh-strength sheet steels with excellent properties are produced on the basis of such knowledge.

1. Introduction

Weight reduction and crash safety considerations have been prompting the use of ultrahigh-strength steel sheet with a tensile strength of over 980 MPa in automobile bodies. Inner and outer white body panels are primarily made of high-strength steels with a tensile strength of 340 to 440 MPa. High-strength steels with a tensile strength of 590 MPa or more are used in automobile structural members that require particularly high strength, such as bumper reinforcements and door impact beams[1,2]. More recently, ultrahigh-strength steels with a tensile strength of more than 980 MPa have come to be used in these applications[3]. Now that crash safety is a top priority, the role of ultrahigh-strength steels is ever increasing in importance.

Ultrahigh-strength steels must meet formability, spot weldability, phosphatability, fatigue strength, and other property requirements as must conventional high-strength steels. In addition, delayed fracture, which was not a critical factor for conventional high-strength steels, must also be considered. It is now clear that ultrahigh-strength steels cannot be properly formed unless their formability is reviewed from angles different from those for conventional cold-rolled steels[4,5].

This report summarizes findings as far obtained about the relationship between microstructure and formability, delayed fracture, and other service properties required of ultrahigh-strength steels. Cold-rolled high-strength steels with a tensile strength of over 780 MPa, equivalent to that of ultrahigh-strength steels, are discussed here.

2. Types of Ultrahigh-Strength Sheet Steels

Table 1 lists the types of cold-rolled ultrahigh-strength sheet

Table 1 Types, chemical compositions, and mechanical properties of automotive ultrahigh-strength sheet steels

Tensile strength	Chemical compositions (mass %)						Mechanical properties		
	C	Si	Mn	P	S	Ti	YP (MPa)	TS (MPa)	El (%)
780MPa	0.06	0.70	2.4	≦0.015	≦0.015	—	620	850	18
980MPa	0.14	0.50	2.4	≦0.015	≦0.015	—	750	1,050	15
1,180MPa	0.14	0.50	2.5	≦0.015	≦0.015	0.05	950	1,250	10
1,370MPa	0.15	0.50	2.7	≦0.015	≦0.015	0.05	1,150	1,420	8

*1 Technical Development Bureau
*2 Nippon Steel Techno Research Corporation
*3 Nagoya Works (presently Yoshikawa Kogyo Co., Ltd.)
*4 Nagoya Works

steels currently used or studied for use by automobile manufacturers. Chemical composition varies with the specifications of the annealing equipment. A small amount of alloying elements suffices for quenching purposes on a continuous annealing line that incorporates a water quenching system. On the other hand, a higher alloy content is required on a continuous annealing line with a gas-water spray cooling system which is slightly lower in the cooling rate. Gas-water mist cooling has the advantage of securing a strip shape, however. Each method has its advantage and disadvantage. This report deals with the ultrahigh-strength steels produced on a continuous annealing and processing line (C.A.P.L.) of the gas-water spray cooling type. The steels listed in **Table 1** are produced on gas-water spray cooling C.A.P.L. lines. Sheet products with a tensile strength of up to 1,370 MPa can be made on the gas-water spray cooling C.A.P.L.. Sheet products with a still higher tensile strength cannot be commercially produced by the C.A.P.L. process because of the problem of delayed fracture discussed later.

Sheet steels are strengthened generally by solid solution, precipitation, and transformation, in the order mentioned following the rise of the required strength level. Ultrahigh-strength steels make use of transformation hardening. Since there is a limit to the carbon content in assuring the desired delayed fracture toughness and spot weldability, precipitation hardened is employed in combination to make up for the lack of strength. **Photo 1** shows the microstructure of a 1,370 MPa ultrahigh-strength steel. The microstructure consists predominantly of bainite and contains martensite as well.

The relationship between the strength and elongation of ultrahigh-strength steels is as shown in **Fig. 1**. The formability of ultrahigh-strength steels is discussed often in terms of elongation[6], but elongation does not always correlate with formability. Formability is very closely related to microstructural homogeneity as described in the next section. The r value of ultrahigh-strength steels is lower than that of conventional mild steel and is about 1.0. If the ultrahigh-strength steel in question has good formability, it can be successfully processed to a drawing ratio of about 2.0 by multiple-step forming.

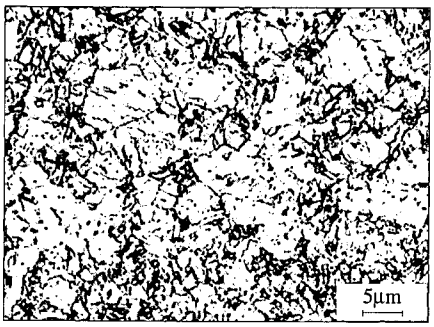

Photo 1 Microstructure of 1,370-MPa ultrahigh-strength steel

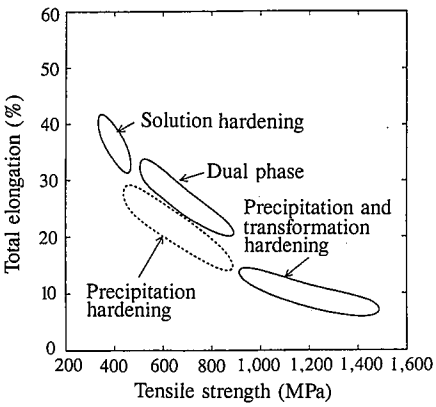

Fig. 1 Relationship between tensile strength and total elongation

3. Properties of Ultrahigh-Strength Sheet Steels

3.1 Relationship between formability and microstructure of ultrahigh-strength sheet steels

Ultrahigh-strength sheet steels are applied to parts which are formed mainly by bending. **Photo 2** shows a door impact beam formed from ultrahigh-strength steel sheet. As seen in this case, many ultrahigh-strength steel parts have hat-shaped cross sections drawn in some parts. To simulate this type of forming, a part of the shape shown in **Fig. 2** was stamped from ultrahigh-strength steel, and its formability was evaluated. Steels of the chemical compositions listed in **Table 2** were annealed under different conditions to provide different levels of yield strength and elongation. Formability was evaluated using specimens with a tensile strength of 1,000 MPa. The effect of total elongation on the forming height is shown in **Fig. 3**(a), and the effect of bendability in **Fig. 3**(b). The total elongation is the elongation of a JIS

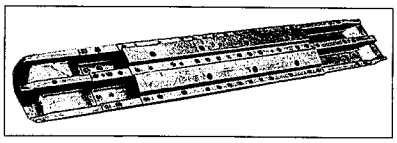

Photo 2 Door impact beam formed from ultrahigh-strength steel

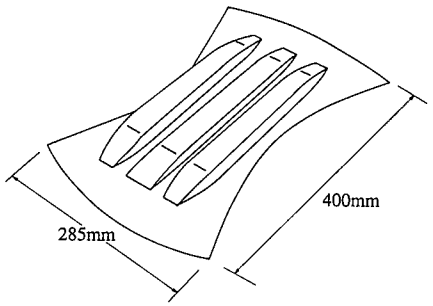

Fig. 2 Shape of model stamped part

Table 2 Chemical compositions of steels

(mass%)

No.	C	Si	Mn	P	S	Al	N	Ti	Nb	B
1	0.09	0.25	2.13	0.011	0.005	0.025	0.0031	0.071	—	—
2	0.12	0.51	1.90	0.013	0.003	0.030	0.0033	0.037	—	—
3	0.13	0.48	2.23	0.015	0.003	0.042	0.0029	0.059	—	—
4	0.13	0.52	2.30	0.014	0.004	0.034	0.0027	0.040	—	0.0015
5	0.14	0.44	1.65	0.016	0.002	0.032	0.0029	—	—	—
6	0.14	0.59	2.26	0.008	0.003	0.024	0.0040	0.045	—	—
7	0.14	0.50	2.66	0.017	0.003	0.030	0.0044	0.098	—	0.0020
8	0.15	0.47	2.66	0.015	0.001	0.024	0.0031	0.002	—	—
9	0.15	0.04	2.39	0.030	0.006	0.036	0.0050	0.001	0.032	—
10	0.16	0.48	2.23	0.012	0.002	0.024	0.0050	0.055	—	—

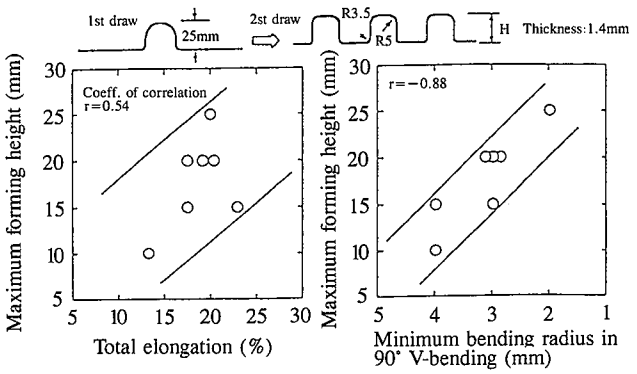

(a) Effect of total elongation (b) Effect of bendability

Fig. 3 Effects of total elongation and bendability on forming height

No. 5 specimen with a gage length of 50 mm as determined in tensile test. Bendability was evaluated by placing a specimen over a 90° V-block, forcing a punch of specified tip radius into the specimen, and measuring the minimum bending radius at which the specimen did not crack. As evident from **Fig. 3**, the formability of ultrahigh-strength steels correlate with bendability better than with total elongation. This means that the formability of ultrahigh-strength steels is governed by the local ductility that can be evaluated by bendability.

To clarify the factors that govern the bendability of ultrahigh-strength steels, its relationship with microstructure was investigated. Ultrahigh-strength sheets with different microstructures were produced by changing first the cooling rate of hot-rolled strip and then the heat treating and annealing conditions. **Photo 3** shows typical microstructures thus obtained.

A homogeneous microstructure is seen in **Photo 3**(a), a heterogeneous lamellar microstructure in **Photo 3**(b), and a heterogeneous microstructure with islands of soft portions in **Photo 3**(c). Hardness was measured at five points at 2 mm intervals from the surface of sheet specimens on the Rockwell C scale, and its standard deviation was taken as a microstructural homogeneity index. Shown respectively in **Figs. 4** and **5** are the effects of the minimum bending radius on the total elongation and the microstructural homogeneity index. It should be noted that the minimum bending radius does not correlate at all with the total elongation but correlates well with the microstructural homogeneity index. The effect of minimum bending radius on tensile strength is shown in **Fig. 6**. Bendability does not correlate with tensile strength, and when tensile strength is high, good bendability can be obtained if microstructural homogeneity is high. This suggests that microstructural homogeneity is an important factor

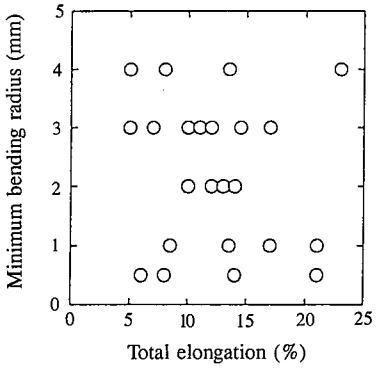

Fig. 4 Effect of minimum bending radius on total elongation

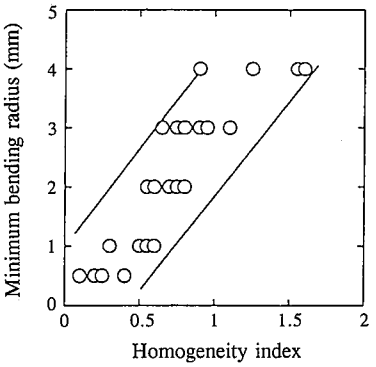

Fig. 5 Effect of minimum bending radius on microstructural homogeneity index

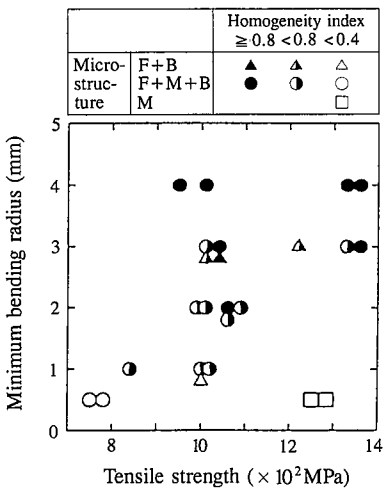

Fig. 6 Effect of minimum bending radius on tensile strength

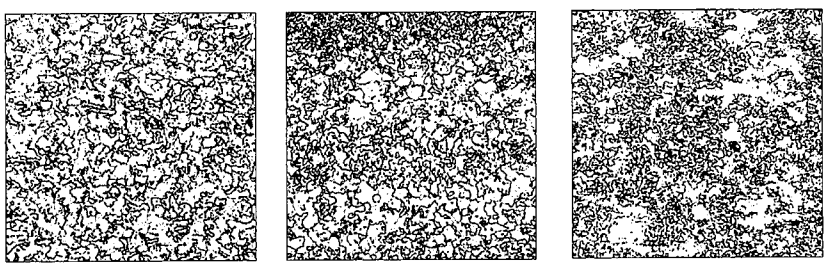

(a) Homogeneous microstructure (b) Heterogeneous lamellar microstructure (c) Heterogeneous insular microstructure

Photo 3 Homogeneous and heterogeneous microstructures of ultrahigh-strength steel

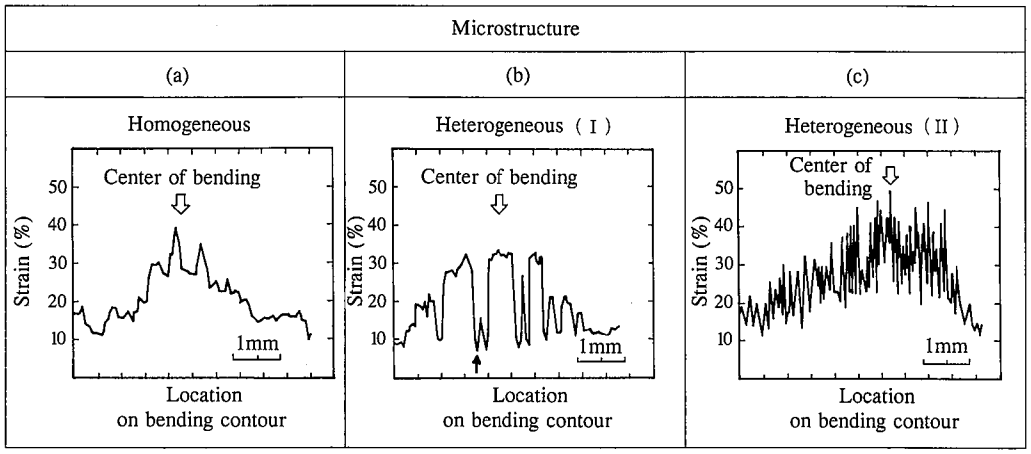

Fig. 7 Strain distribution of steel sheet surface after 90°V bending

governing the formability of ultrahigh-strength steels.

The strain distribution of the bend surface was measured to examine in detail the relationship between microstructural homogeneity and bendability. The steel sheet surface was etched in an oxalic acid solution to reveal grain boundaries. A given grain boundary was used as gage mark, and the strain distribution of a minute portion over a gage length of about 50 μm was determined. The measurement results are shown in **Fig. 7**. When a heterogeneous microstructure is bent, it reveals portions of extremely low strain compared with a homogeneous microstructure. Low-strain portions are present at long intervals in the heterogeneous lamellar microstructure of **Photo 3**(b) and at short intervals in the heterogeneous insular microstructure of **Photo 3**(c). High-strain portions are composed predominantly of ferrite, and mild and ductile, while low-strain portions are predominantly of martensite, and hard. Bending-induced cracking occurs at the boundary between soft and mild portions as indicated by the arrow in **Fig. 7**(b), or within a hard layer. In a steel of a heterogeneous microstructure, strain does not uniformly propagate, high-strain portions are locally produced, and cracks are initiated at boundaries between the high-strain portions and the surrounding low-ductility portions. The end result is a decrease in bendability.

Formability has been discussed above, centering on bendability. The above discussion applies also to stretch flangeability. To evaluate the stretch flangeability of ultrahigh-strength steels, the hole expansion ratio was measured by the method shown in **Fig. 8**. **Fig. 9** shows the effects of the hole expansion ratio on the total elongation and microstructural homogeneity index. If the steel has a good hole expansion ratio, its microstructural homogeneity increases at the sacrifice of total elongation. In other words, microstructural homogeneity has a greater impact on the stretch flangeability of ultrahigh-strength steel than total elongation does. A homogeneous microstructure such as single-phase bainite, rather than a duplex microstructure, is generally said to enhance stretch flangeability. Macrostructural homogeneity is also important for steels of still higher strength.

From the above discussion, it can be said that the formability of ultrahigh-strength steels is governed by the local ductility that can be evaluated by bendability, and can be significantly improved through microstructural homogenization.

3.2 Delayed fracture

When strength exceeds 1,000 MPa as is the case with ultrahigh-strength cold-rolled steels, delayed fracture tends to occur. Delayed fracture is a phenomenon that a formed part, which is sound immediately after forming, cracks after some time. This phenomenon is well known for austenitic stainless steels[7], but has been seldom observed in ferritic steels like conventional cold-rolled sheet steels.

Photo 4 shows the occurrence of delayed fracture. Ultrahigh-strength steels of the chemical compositions listed in **Table 2** were annealed at different temperatures, deep drawn into cups with a drawing ratio of about 2.0, immersed in ethyl alcohol, and caused to develop delayed fracture. **Fig. 10** shows the relationship between the time of immersion in ethyl alcohol and

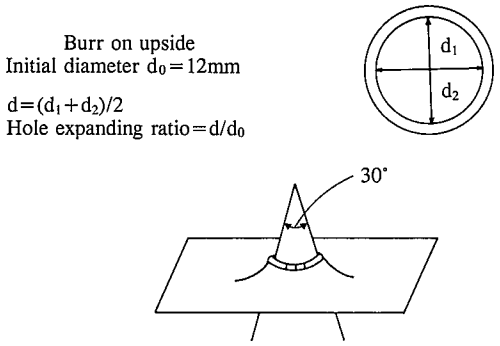

Fig. 8 Hole expansion test method

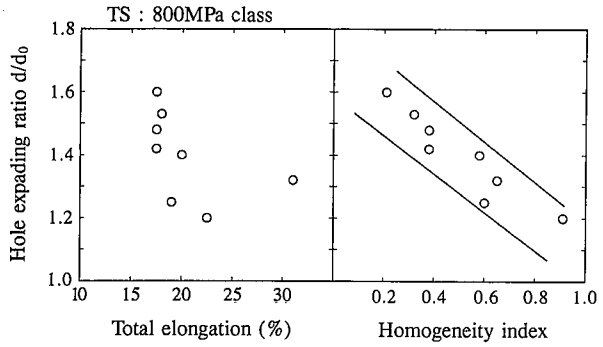

Fig. 9 Effects of hole expansion ratio on total elongation and microstructural homogeneity

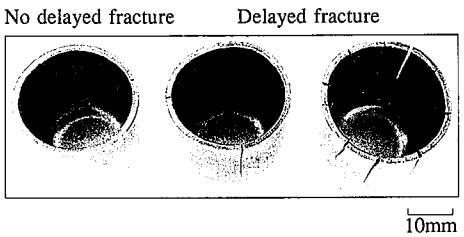

Photo 4 Delayed fracture

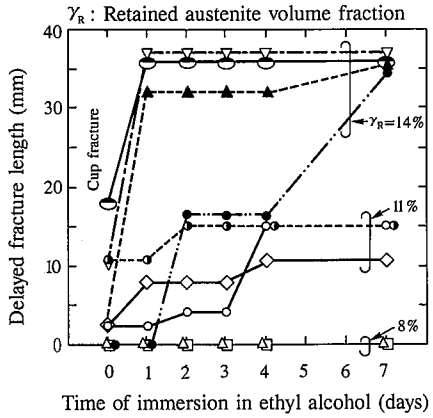

Fig. 10 Propagation of delayed fracture

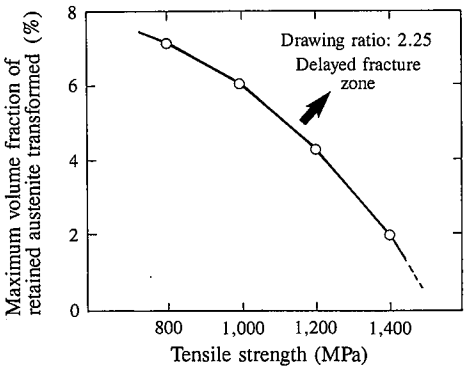

Fig. 11 Relationship between tensile strength and volume fraction of forming-transformed austenite, both affecting delayed fracture of ultrahigh-strength steels

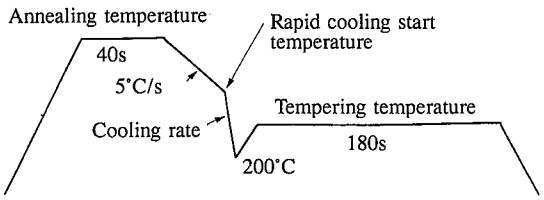

Fig. 12 Annealing cycle

the total length of delayed cracking. When the test results are stratified by the volume fraction γ_R of retained austenite, the larger the retained austenite volume fraction, the greater the delayed cracking tendency. The retained austenite volume fraction was determined by comparing the X-ray diffraction intensities of the (200), (220), and (311) planes of austenite with those of standard specimens. Sheets for which the retained austenite volume fraction were measured beforehand were drawn into cups. A specimen was machined from the wall of each cup. The austenite volume fraction of the specimen was measured, and then the forming-induced reduction of the austenite volume fraction, that is, the volume fraction of austenite transformed by forming was measured. To know the relationship between the volume fraction of austenite transformed by the forming and the delayed fracture tendency, the maximum transformed austenite volume fraction of specimens that did not crack when immersed in ethyl alcohol for 7 days was measured. The relationship between this retained austenite volume fraction and the tensile strength of the sheet specimens is shown in **Fig. 11**. From this figure, it can be seen that the limit volume fraction of austenite to the occurrence of delayed fracture decreases with increasing tensile strength. Since the austenite whose volume fraction is reduced by the cupping is considered to have been transformed to martensite by forming, the volume fraction of forming-induced martensite has an effect on the delayed fracture of ultrahigh-strength steel. When the steel has a high retained austenite volume fraction, shrink flange cracks occur in deep cup drawing alone. The volume expansion that accompanies the forming-induced transformation produces internal stress, which in turn causes a delayed fracture in the ultrahigh-strength steel. If the retained austenite volume fraction is so small that no cracks occurs when the steel is formed, many flaws are produced at grain boundaries with the adjoining phase. Under these circumstances, atomic hydrogen is considered to easily accumulate, turn into molecular hydrogen, and induce the delayed fracture of the steel. Hydrogen is reported to infiltrate from the press forming lubricant[7] and is also considered to come from the rust-preventive oil applied to the sheet. The coating and painting processes are other probable sources of hydrogen. In the martensite phase, hydrogen is high in the diffusion rate and low in solubility. The hydrogen that enters and accumulates in the martensite phase easily deposits at boundaries with the other phase.

The maximum austenite volume fraction at which delayed fracture occurs increases as the tensile strength of the steel decreases. This is probably because when the steel strength is low, the phase surrounding the retained austenite is so high in deformability that it deforms to reduce the number of phase-boundary defects or the residual stress, even if the austenite transforms and its volume expands under the forming. The minimum tensile strength at which delayed fracture actually becomes a problem is put at 1,200 MPa. The way the delayed fracture of cups occurs is shown in **Photo 4**. A crack occurs to release local macroscopic residual stress, only to be followed by another crack elsewhere. Four or more cracks are eventually caused in some cups. This indicates that the occurrence of delayed cracking is governed by the residual stress acting between microconstituents, rather than macroscopic residual stress.

3.3 Effects of manufacturing conditions on delayed fracture

As discussed above, it was confirmed that microstructural homogeneity and reduced retained austenite volume fraction are important factors in formability and delayed fracture, respectively. Study was now made of the manufacturing conditions necessary to achieve these targets. **Figs. 13** through **16** show the effects respectively of the annealing temperature, cooling rate, rapid cooling start temperature, and tempering temperature in the annealing cycle of **Fig. 12** on the retained austenite volume frac-

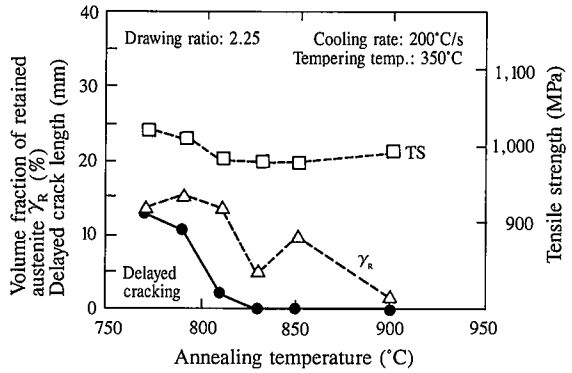

Fig. 13 Effect of annealing temperature on delayed fracture

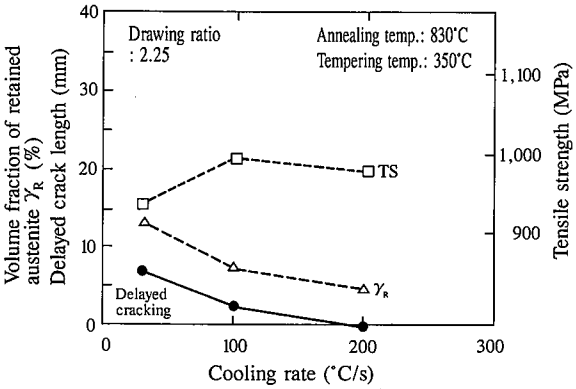

Fig. 14 Effect of cooling rate on delayed fracture

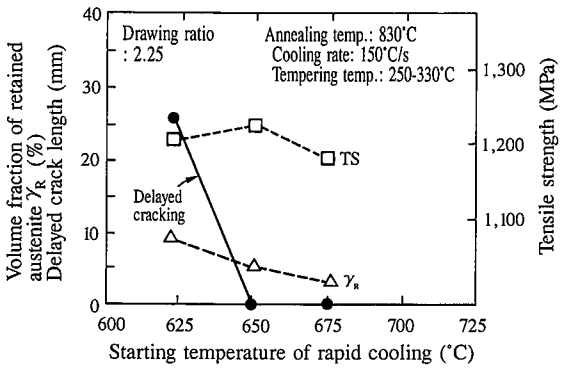

Fig. 15 Effect of rapid cooling start temperature on delayed fracture

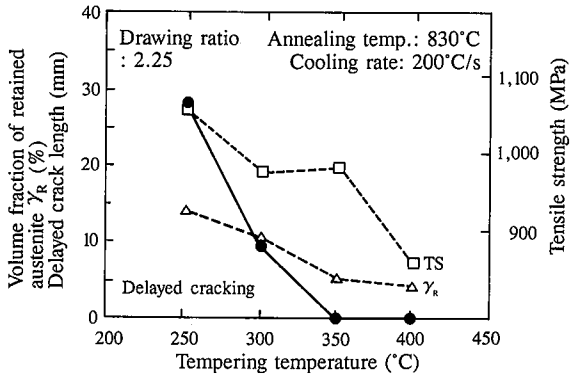

Fig. 16 Effect of tempering temperature on delayed fracture

tion and delayed crack length.

The delayed fracture tendency decreases as the annealing temperature rises, and delayed fracture does not occur at all when the annealing temperature exceeds 830°C. This is because increasing the annealing temperature increases the austenite ratio and decreases the carbon enrichment, making it difficult for the austenite to remain after rapid cooling. Annealing at temperatures above the A_3 transformation temperature equalizes the carbon concentration, which in turn causes the lamellar microstructure to disappear and improves the formability of the steel. The lower the cooling rate, the lower the delayed fracture tendency. This is because rapid cooling shortens the time for passage through the two-phase region, inhibits the carbon enrichment, and retards the formation of retained austenite. A high rapid cooling start temperature is preferred, also because the time spent in the two-phase region in the cooling process is shortened. A tempering temperature of over 350°C is desirable, because it helps to transform retained austenite to martensite and to recover the ductility of martensite. The entrapment of hydrogen in carbides is known to prompt delayed fracture, and the low-temperature tempering under which carbides decrease is reported to be effective in preventing delayed fracture[8]. In the case of **Fig. 16**, however, the steel tempered at 250°C, a temperature at which the formation of carbides is small, has a greater delayed fracture tendency. Retained austenite is thus considered to have a significant effect on the delayed fracture of sheet steel. **Fig. 17** shows the delayed fracture occurrence tendency when the carbon content is changed. A 90 mm long, 30 mm wide, and 1.6 mm thick sheet specimen was bent to a radius of 10 mm, bolted at one end, and immersed in a 5% dilute sulfuric acid solution as subjected to a stress of 590 MPa and current density of 0.15 A/cm^2. The time to the occurrence of delayed cracking in the specimen under these conditions was measured. As indicated, the time to the occurrence of delayed fracture steeply decreases as the carbon content exceeds 0.20%.

From what has been discussed above, it may be said that the manufacturing conditions to ensure the desired formability and delayed fracture resistance in ultrahigh-strength steels are annealing at a temperature above the A_3 transformation temperature, rapid cooling from as high a temperature as possible, and tempering at a temperature of 350°C or more.

Since delayed fracture occurs when the carbon content exceeds 0.20% as shown in **Fig. 17**, the maximum carbon content should be held under 0.20%. The maximum carbon content of ultrahigh-strength steels in commercial production is about 0.16%.

Ultrahigh-strength steels are produced with satisfactory formability and delayed fracture resistance by adopting appropriate manufacturing conditions as discussed above.

3.4 Spot weldability

The spot weldability of high-strength steel sheets has been studied by many researchers[9]. Results generally obtained are as follows: 1) optimum welding conditions are high electrode force and low welding current; 2) tensile shear strength varies approximately with the tensile strength of base metal, but cross tension strength does not; and 3) use of precipitation hardening elements are effective in preventing cross tension strength from dropping. **Fig. 18** shows the spot weldability of ultrahigh-strength steels with the chemical compositions listed in **Table 1**. As proved in previous spot weldability test results, the tensile shear strength of

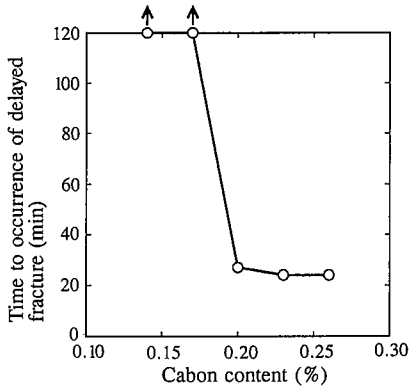

Fig. 17 Effect of carbon content on delayed fracture

spot welded joints varies with the tensile strength of base metal, but the cross tension strength does not rise as much as the tensile strength of base metal does. As the tensile strength of base metal rises, the cross tension strength of spot welded joints does not appreciably decline because precipitation-hardening elements are added. As the loss of strength may sometimes be greater than in

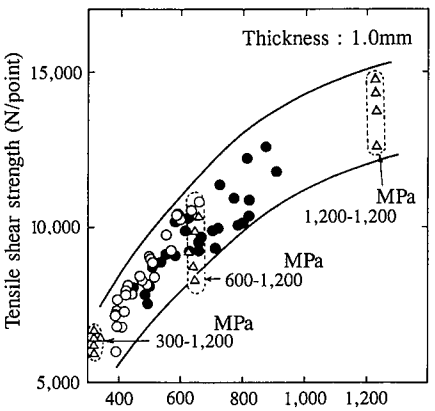

(a) Tensile shear strength of spot welded joint versus tensile strength of base metal

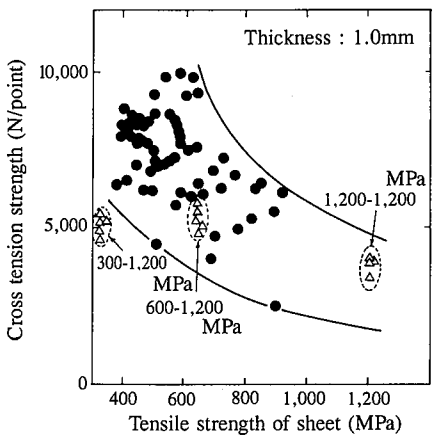

(b) Cross tension strength of spot welded joint versus tensile strength of base metal

Fig. 18 Tensile strength of spot welded joints

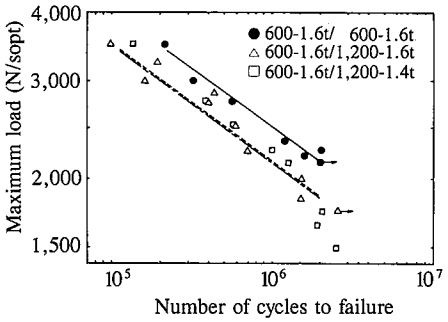

(a) Tensile shear fatigue strength

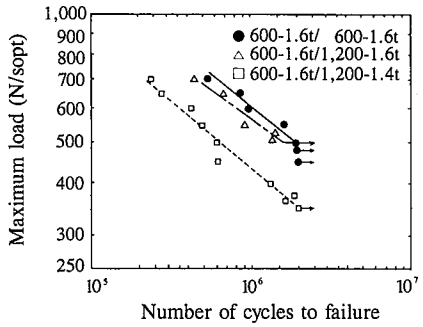

(b) Cross tension fatigue strength

Fig. 19 Fatigue strength of spot welded joints

mild steel sheets, however, the number of spot welds must be increased, or some other remedial measures must be taken for such a mode as cross tension, in which the load is applied normal to the sheet surface. Such considerations are already in practice in the resistance spot welding of ultrahigh-strength steels.

The fatigue strength of spot welded joints is as shown in **Fig. 19**. The results of **Fig. 19** are those obtained when ultrahigh-strength steel sheet was spot welded in combination with lower-strength steel sheet, considering application to actual parts. The 1,200-600 MPa combination provides approximately the same fatigue strength as the 600-600 MPa combination. The sheet thickness, however, greatly influences the fatigue strength of spot welded joints. The effect of thickness must be taken into account when spot welding ultrahigh-strength sheet together with lower-strength sheet.

3.5 Other properties

Phosphatability deteriorates with increasing silicon content, but this deterioration of phosphatability is known to be small when the manganese content is high[10]. The ultrahigh-strength steels listed in **Table 1** have had no problem with phosphatability.

The plane-bending fatigue limit ratio of ultrahigh-strength steels is 0.40 to 0.45 and is comparable to that of conventional precipitation-strengthened steels.

Cold-work embrittlement was evaluated by drawing a 60 mm diameter blank into a cup with a drawing ratio of 2.0, applying an impact load to the cup at the specified temperature, and determining the transition temperature at which the cup cracked. **Fig. 20** shows the relationship between the transition temperature and the retained austenite volume fraction. If the retained austenite volume fraction is low, 1,400 MPa ultrahigh-strength steels

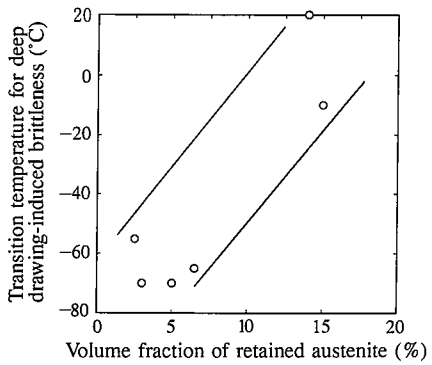

Fig. 20 Cold-work embrittlement of ultrahigh-strength steels

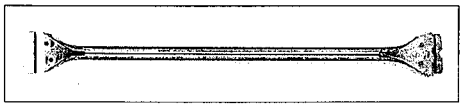

Photo 5 Door impact beam formed from ultrahigh-strength steel

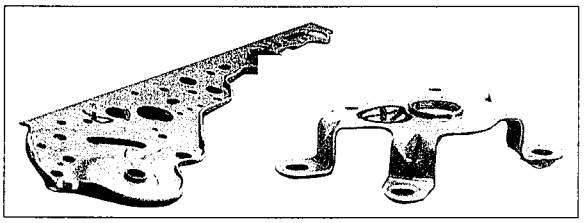

Photo 6 Seat parts formed from ultrahigh-strength steel

exhibit an excellent transition temperature of −55°C or less.

4. Application to Automobile Parts

Automobile parts formed from ultrahigh-strength steels are shown in **Photo 5** and **6**. **Photo 5** shows a door impact beam formed from a 1,200 MPa ultrahigh-strength steel. The steel was produced with necessary considerations about formability and delayed fracture for this application. **Photo 6** shows seat parts formed from a 800 MPa high-strength steel. A dual-phase steel with good total elongation and a steel with low total elongation but with stretch flangeability improved by microstructural homogenization were tried as candidate materials for seat parts. The latter steel yielded far better formability and was selected as the material for seat parts. As shown in this example, it is important not only to focus on the total elongation, but also to improve formability by homogenizing the microstructure.

5. Conclusions

Findings obtained to date have been summarized about the relationships between the mechanical properties and the microstructures and manufacturing conditions of ultrahigh-strength steels used in automobile parts. That is, the formability of ultrahigh-strength steels is governed by the local ductility that can be evaluated by bendability, and can be improved by homogenizing the microstructure. The delayed fracture tendency can be reduced to a practically acceptable level by reducing the volume fraction of retained austenite by high-temperature annealing, for example. Ultrahigh-strength steel sheets that specifically meet phosphatability, spot weldability, base-metal and weld-metal fatigue strength, cold-work embrittlement, stretch flangeability, and other properties can be produced by optimizing the alloy design and manufacturing conditions. According to these findings, high-performance ultrahigh-strength steels are produced and applied. Given the importance of accomplishing automobile weight reduction and crash safety at the same time, ultrahigh-strength steels will see widespread use in increasing automotive applications.

References

1) Rashid, M.S.: SAE Paper. 760206, Detroit, 1976
2) Baily, D.J.: SAE Paper. 760715, Dearborn, 1976
3) Shiroi, Y., Niwa, S., Iwata, T.: Journal of JSAE. 42 (6), 761 (1988)
4) Yamazaki, K., Mizuyama, Y., Oka, M.: CAMP-ISIJ. 5 (6), 1839 (1992)
5) Oka, M., Takechi, H.: Formability and Metallurgical Structure. The Metallurgical Society Inc. 1986, p. 83
6) Miyahara, M., Shirasawa, H., Tanaka, Y., Baba, Y.: Kobe SteelEngineering Reports. 35 (4), 92 (1980)
7) Arakawa, M., Sumitomo, H.: J. Jpn. Soc. Technol. Plast. 9 (205), 148 (1978)
8) Nagataki, Y., Tsuyama, S., Hosoya, Y., Ohkita, T.: CAMP-ISIJ. 6 (3), 688 (1993)
9) Hanai, S., Sato, T.: J. Jpn. Soc. Technol. Plast. 15 (166), 885 (1974)
10) Maeda, S., Asai, T., Arai, S., Suzuki, K.: Tetsu-to-Hagané. 68 (16), 2497 (1982)